Advances in Astrophysics, Vol. 5, No. 3, August 2020
https://dx.doi.org/10.22606/adap.2020.53002

Properties of Infrared Source Based on the Big Data of LAMOST Spectral Survey

Le Tian[1,2*], ZhongZhong Zhu[1,2], Liyun Zhang[1,2] and Shuai Wang[1,2]

[1]College of Science&College of big data and information engineering, Guizhou University, Guiyang 550025, P. R. China
[2]College of big data and information engineering, Guizhou University, Guiyang 550025, P. R. China
Email: liy_zhang@hotmail.com

Abstract Big data of the spectroscopic survey of the Large Sky Area Multi-object Fiber Spectroscopic Telescope (LAMOST) are important for studying the properties of infrared source. We obtained 5946 spectra of 4843 infrared stars through cross matching of LAMOST DR3 and WISE. We measured the equivalent widths of the Hα line and other Balmer lines, Ca II H and IRT lines. According to the EWs of Hα lines, we found there are 390 spectra of 294 infrared stars showing strong activity. We found that 77 spectra were first observed by LAMOST. We found 36 objects show chromospheric activity variation in the Hα emission line. In the end, we gave the physical mechanism of the early-type stars and late-type stars activity.

Keywords: infrared source, stars, stellar chromospheric activity, LAMOST

1 Introduction

In the Universe, the objects radiating in the infrared band are called infrared sources. There are lots of dust, atoms and molecules in the interstellar space. The main reason for interstellar extinction is that these substances will scatter and absorb electromagnetic radiation, and the dust is the most significant. The observation has shown that the selection of the interstellar extinction wavelength is more significant the ultraviolet and visible light than the infrared extinction. On this account, infrared observation objects that are more faint has more advantages.

The star also has infrared radiation in the process of evolution. The typical star-forming region are infrared dark clouds, IRDCs. It is considered as a massive star-forming region (Rathborne et al., 2006; Peretto et al., 2010). IRDCs are cold, highly invisible, dense molecular clouds, which are firstly observed in the bright background disappearance in infrared galaxy (Perault et al., 1996; Egan et al., 1988). When the star evolves to the pre-main sequence and main sequence star stages, its infrared radiation is mainly from the circumstellar dust disk and planet disk. The radiation of the dust received from the central star is in the infrared band. The observation proves that the circumferential disk around the main sequence star is a common phenomenon, IRAS unexpectedly found infrared excess around in Vega (Aumann et al., 1984). Using the observation results of IRAS, Oudmauher (1992) found 462 infrared excess in the SAO star table and verified that the celestial bodies have PMS, Be, AGB and the original planetary systems. Rhee (2007) selected 160 infrared excess from the IRAS observation database to select debris disk distance about 120 pc. The spectra of the central celestial bodies are mostly early-type stars of B-F and only a few of them are late type star.

Yet the most interesting thing was stellar magnetic activity and chromospheric activity. The rule of its activities will produce a set of emission lines in the spectrum of stars, representative of the Balmer line, Ca II H&K, and Ca II infrared triple line. It is generally believed that the magnetic reunion and the deep convection are the reasons for this phenomenon (Zhang et al., 2015; Vida et al., 2015; Zhang et al., 2016; Montes & Crespo-chacón, 2004). Catalano (1998) revealed the relationship between the Hα and Ca II lines according to solar results. Frasca (2016) calculated the Hα and Ca II IRT fluxes of cool stars (T_{eff} $\leq$6000K) have found 442 the chromospheric of active stars. Yi et al. (2014) found 1971 Hα active star from 58360 M dwarfs in the LAMOST pilot survey. Therefore, it is of great significance to study the spectral properties of the stars in understanding the magnetic activity and chromospheric activity.

We introduced the LAMOST and WISE survey and data screening in the section 2. Spectral analysis of richly active and poorly active of stars are in section 3. It is also in this part of the spectral type of statistics. In the section 4, we summarized our results.

2 Data

2.1 LAMOST and WISE Survey

The Large Sky Area Multi-Object Fiber Spectroscopic (LAMOST, also called the Guo Shou Jing Telescope) with a large aperture and wide field adopts an innovative active optics technique (Cui et al., 2012). It is located in Xinglong observation station of National Astronomical Observatories Of China (NAOC). The unique design of LAMOST enables it to take 4000 spectra in a single exposure at a limiting magnitude as faint as r=19 at the resolution R=1800, which is equivalent to the design aim of r=20 for the resolution R=500 (Zhao et al., 2012). At the beginning of the design, the LAMOST was appointed to the two main tasks: the LAMOST Extra Galactic Survey (LEGAS) and the LAMOST Experiment for Galactic Understanding and Exploration (LEGUE) survey of MilkyWay stellar structure. Its appearance effectively promotes international exchanges and cooperation in the field of astronomy.

The LAMOST pilot survey released 906420 spectra totally, containing 807575 stars. Its formal regular survey launched on September 28, 2012 (Luo et al., 2012). The data set of LAMOST data released three (DR3), there are 1622344 total spectral, containing 1489013 stars. In this paper, we found active stars in the stellar catalog of the DR3.

The wide-field Infrared survey Explorer, known as WISE (Wright et al., 2010), is a highly sensitive, all-day sky survey telescope launched by NASA on Dec. 14, 2009. From January 14, 2010 to July 17, 2010, it completed its first round of patrol, with a central wavelength of 3.4, 4.6, 12 and 22 microns, with a corresponding resolution of 6.1, 6.4, 6.5, 12 arcseconds, sensitivity 0.08, 0.1, 1 and 6 mJy, the source location accuracy of high SNR is even 0.15 arcseconds. WISE works in the mid-infrared band, making many contributions to find young stars. Koenig (2012) identified 3 open clusters and 11 outer Galaxy massive star-forming regions from WISE's survey data and counted the distribution of these young stars in each region. Koenig (2015) had certified 418 stars in σ Orionis and 544 stars in λ Orionis from the WISE-2MASS catalogs of YSO candidates.

2.2 LAMOST and WISE Cross-Certification

In this section, we will introduce the data selection process. Our purpose is to find active stars through data cross-certification released by the LAOMST DR3 and the WISE all-sky survey. As described above, the LAOMST DR3 have 1489013 stars. And the WISE all-sky survey released 345165 infrared source, which contains 158114 stars, 145905 galaxies and 41146 other types of celestial bodies. The key of cross-certification is that the observation coordinates of the same source of two telescopes are within the error range. Therefore, the error of the rectascension and the declination was set in less than 2 degrees. Through such process, we found 3762 stars in infrared stellar catalog and found 2184 stars in infrared galactic. The LAMOST identified the objects by doing spectrum of $3700\text{Å} < \lambda < 9100\text{Å}$ (zhao et al., 2012; Cui et al., 2012), and the WISE is photometry in W1 W2 W3 W4 of mid-infrared and far-infrared (Wright et al., 2010). By contrast, the LAMOST identifies more accurately. According to the spectral characteristics exhibited by active stars, that is the Hα, Hβ, Hδ, Hγ and Ca II H&K, Ca II IRT, we obtained 390 spectral of active stars from LAMOST's 5946 spectrum. We showed some cross-certification data in Table 1.

3 Discussion

3.1 Active Indicators

The 390 spectra provided by LAMOST, not all of them, are all characteristic spectral lines of stellar activity. Depending on the nature and extent of the activity of the star, the emission lines on the spectrum vary in degree. Therefore, we chose 8 spectrum of active stars to show, which is signal-to-noise

Table 1. LAMOST and WISE cross-certification

LAMOST name	WISE name	Spectral S/N	Spectral type	LAMOST Class	WISE Class
J000013.42+402929.7	J000013.43+402929.7	710.51	M1	star	star
J000013.42+402929.7	J000013.43+402929.7	488.93	M1	star	star
J000013.42+402929.7	J000013.43+402929.7	618.29	M1	star	star
J000013.92+373735.0	J000013.93+373735.1	677.61	M1	star	galaxy
J000014.01+373735.2	J000013.93+373735.1	251.97	M0	star	galaxy
J000016.56+445819.4	J000016.46+445819.4	96.43	M7	star	star
J000053.81+050500.2	J000053.81+050500.2	3.19	M0	star	galaxy
J000055.74+175204.4	J000055.75+175204.3	725.96	bad	star	star
J000109.35+425412.2	J000109.04+425412.0	82.4	M2	star	star
J000112.28+430131.3	J000111.94+430131.3	97.17	K5	star	star
J000219.16+125818.1	J000219.14+125818.1	45.38	K2	star	galaxy
J000219.16+125818.1	J000219.14+125818.1	65.68	K4	star	galaxy
J000221.87+042937.7	J000221.65+042937.8	258.78	M2	star	star
J000228.06+414202.5	J000228.06+414202.6	51.46	F2	star	star
J000230.94+382639.3	J000230.92+382639.3	253.48	M2	star	star
J000253.70+545257.7	J000253.70+545257.7	109.23	K4	star	galaxy
J000307.65+553345.7	J000307.27+553346.5	20.3	M2	star	star
J000309.51+440930.8	J000309.52+440930.7	50.47	M6	star	star
J000314.92+160843.0	J000314.90+160843.2	13.99	M1	star	galaxy
J000333.98+263859.8	J000334.00+263900.0	16.6	bad	star	galaxy
J000336.27+032006.5	J000336.26+032006.6	3.09	K7	star	galaxy
J000348.79+472927.0	J000348.79+472927.1	689.29	K7	star	star
J000350.15+102703.6	J000350.22+102703.9	480.74	M2	star	star
J000412.98+104726.0	J000412.96+104726.1	24.61	K3	star	galaxy
J000412.98+104726.0	J000412.96+104726.1	20.52	K4	star	galaxy
J000415.54+331821.3	J000415.52+331821.6	6.6	bad	star	galaxy
J000420.07+400635.8	J000419.99+400634.7	576.09		star	star
J000451.74+120702.2	J000451.74+120702.3	2.35	M2	star	star
J000548.58+420211.8	J000548.84+420213.0	165.89	M5	star	star
J000551.15+405739.4	J000551.15+405739.4	468.33	M1	star	star
J000552.62+550203.7	J000552.63+550201.5	211.58	M6	star	star
J000601.03+162707.6	J000601.06+162707.5	696.28	bad	star	star
J000601.07+162707.6	J000601.06+162707.5	496.78	bad	star	star
J000610.90+365419.3	J000610.89+365419.7	249.29	M3	star	star
J000617.12+351113.7	J000617.12+351113.7	3.36	M0	star	galaxy

Note:Here we show only partial data, and the rest of the data will be uploaded to the web

ratio and the emisson line is obvious. Figure 3 shows the four infrared source spectra of single observation LAMOST J043157.79+182136.9 LAMOST J051645.45-015122.3 LAMOST J053243.05+122108.4 LAMOST J053913.00-012721.2. Figure 5 shows four infrared source spectra of multiple observations LAMOST J000936.85+374731.9 LAMOST J043029.61+242644.9 LAMOST J040559.62+295638.2 LAMOST J065311.55+113256.3.

3.2 Stellar Active Statistics

Active stars range from early stars to late stars. In order to find the law of the active star, we should have been carrying out the statistics of infrared stars. Figure 1 shows that we get the histogram of infrared star statistics. From figure 1, the infrared stars are later than the early stars. Through cross-certification, we obtained 15 B-type stars (4 of them are active), 97 A-type stars (21 of them are active), 251 F-type stars (21 of them are active), 581 G-type stars (27 of them are active), 1361 K-type stars (39 of them are active) and 2667 M-type stars (231 of them are active). In terms of data, whether it's active or not, infrared stars have gradually increased from early stars to late stars, and have the most M-type stars. So this paper mainly discusses the active infrared star optical properties and its chromospheric activity, we do not have an in-depth discussion at one point. It requires more statistical data to prove whether infrared stars have this rule. We shows in figure 2 that the percent of each type of active stars to obtain more in-depth understanding, in which B-type stars are 1.23 percent, A-type stars are 6.46 percent , F-type stars are 6.46 percent , K-type star are 8.31 percent , G-type star are 12 percent, M-type star are 65.54 percent in all the active infrared stars. Why are M-type star so much? Deep convective zones and fast rotation in the chromosphere of many late-type stars produce plages or flares. This phenomenon easily produce balmer lines and Ca II H&K, Ca II IRT lines to explain active M-type star so much (Zhang et al., 2015; Zhang et al., 2016; Vida et al., 2015; Montes & Crespo-chacón, 2004).

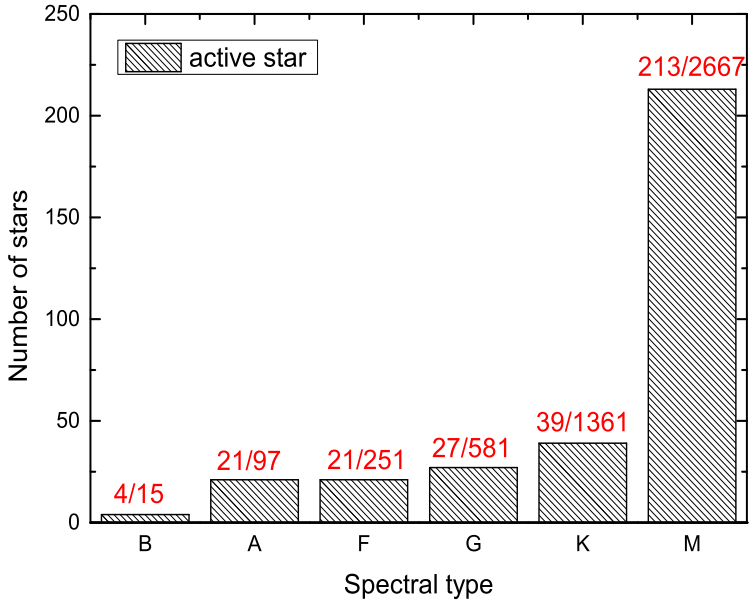

Figure 1. Distribution and proportion of active star with spectral type

3.3 Active Stars Survey

The hammer program made by IDL code (Covey et al., 2007) have assigned stellar spectral types, like SDSS. After that, it has been widely adopted by many researchers to match the spectral type of stars

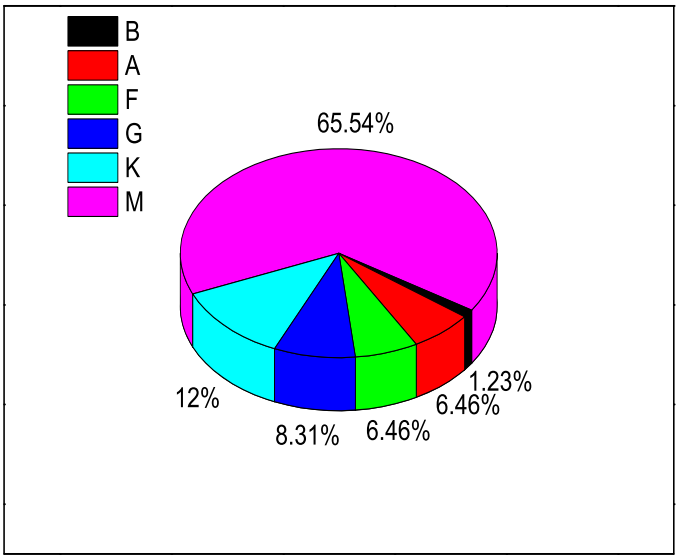

Figure 2. Respectively proportion of each type of active stars

(Zhang et al., 2016; Yi et al., 2014; Lee et al., 2008; West et al., 2011; Woolf & West, 2012; Dhital et al., 2012). The hammer program is also used. We identified the spectral types of 390 stars and calculated the equivalent width of the Hα line (Hawley et al., 2002; Covey et al., 2007; Zhang et al., 2016). We set the SNR more than 3 in this program. In the hammer program, EWs are calculated by integrating the region of 8Å wide centered on the Hα line and subtracting away the mean background flux of two adjacent continuum regions (6555-6560Å and 6570-6575Å).

In the Table 2, we shows that infrared source observed with LAMOST. Each of these columns is LAMOST name (Col(1)), date (Col(2)), the S/N in LAMOST ugriz bands (from Col(3) to Col(7)), the magnitudes in WISE W1 W4 bands (from Col(8) to Col(11)), spectral type (Col(12)), research situation (Col(13)), reference (Col(14)), respectively. "-" of the (Col(14)) represented that this infrared source has not been researched in the literature and that is the firstly obtained by the LAMOST. We found that 77 of 390 spectrum firstly observed by looking at the literature. But they have repeated observations of the same source. There are only part of data in Table and the rest of data will be published in electric format.

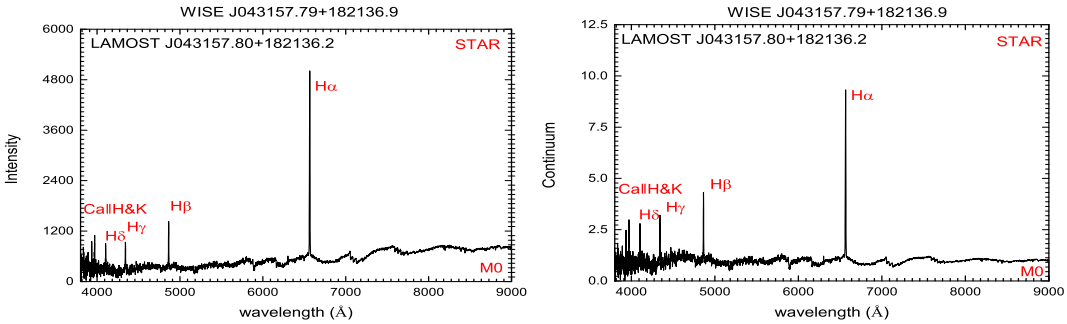

(a) LAMOST J043157.79+182136.9

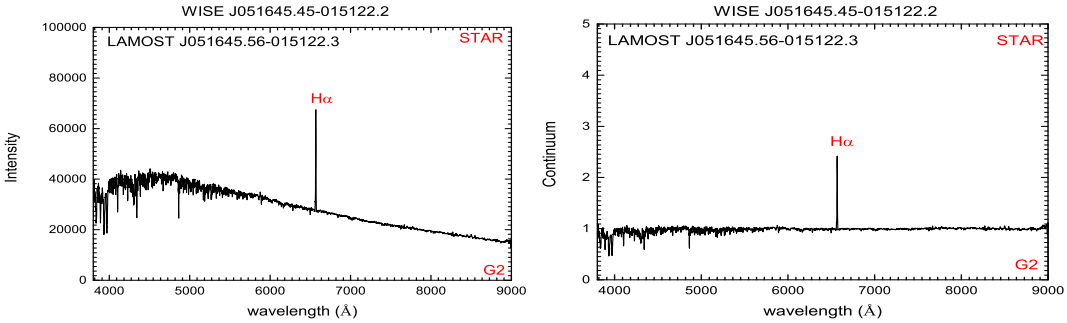

(b) LAMOST J051645.45-015122.3

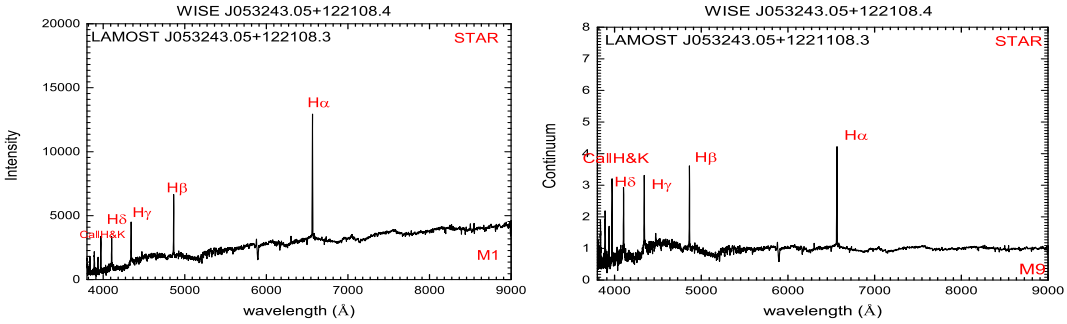

(c) LAMOST J053243.05+122108.4

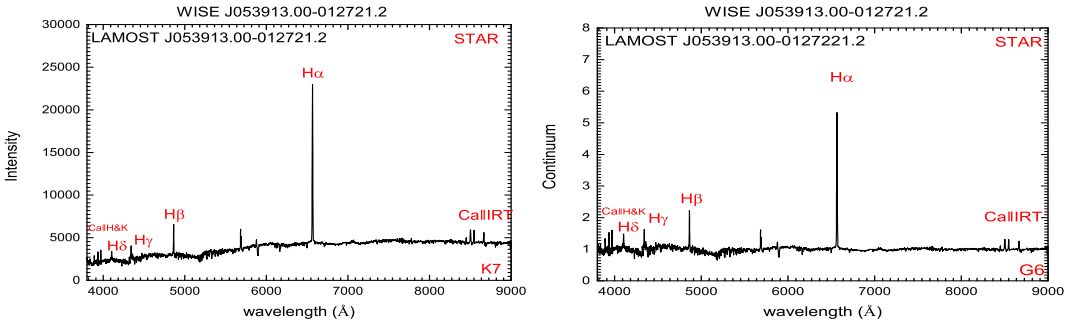

(d) LAMOST J053913.00-012721.2

Figure 3. The spectrum of active infrared stars have H alpha line

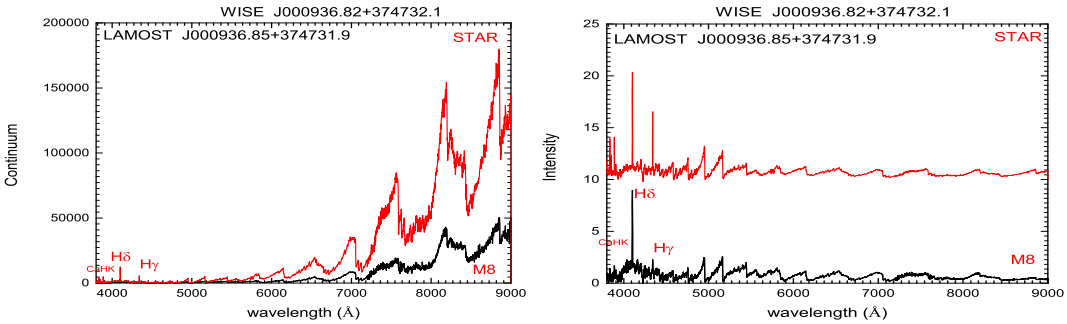

(a) LAMOST J000936.85+374731.9

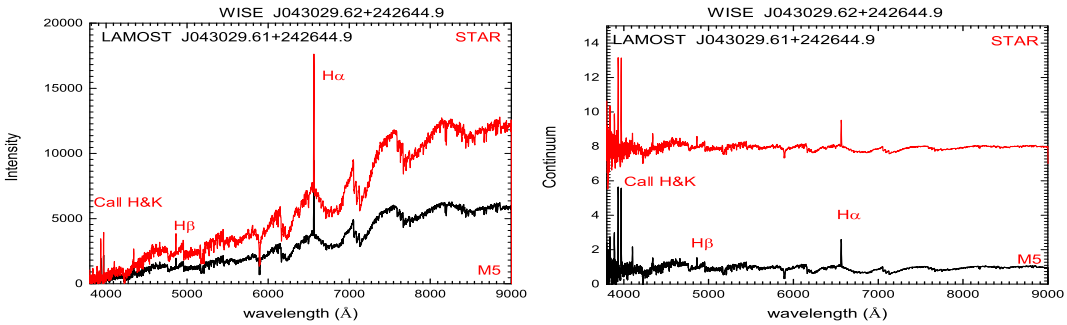

(b) LAMOST J043029.61+242644.9

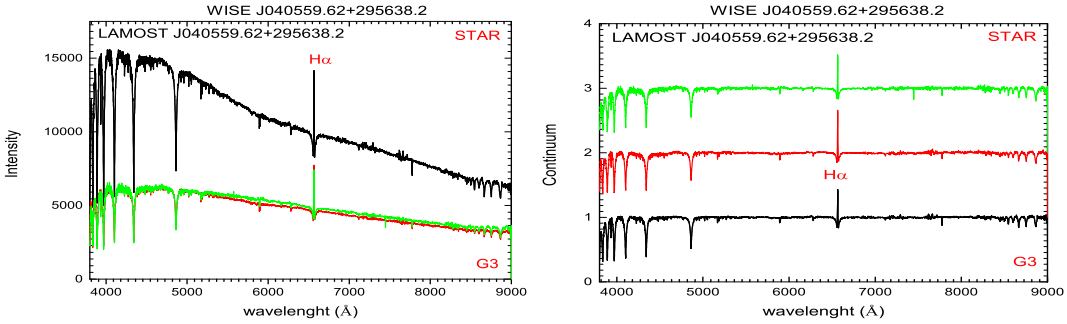

(c) LAMOST J040559.62+295638.2

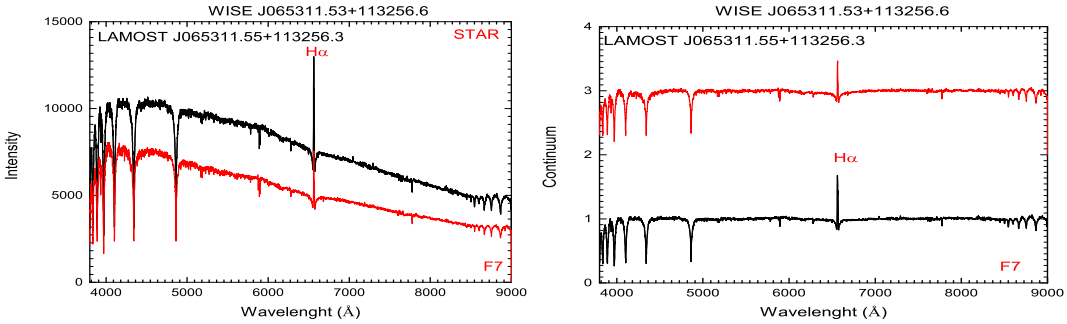

(d) LAMOST J065311.55+113256.3

Figure 4. The spectrum of active infrared stars have twice observations

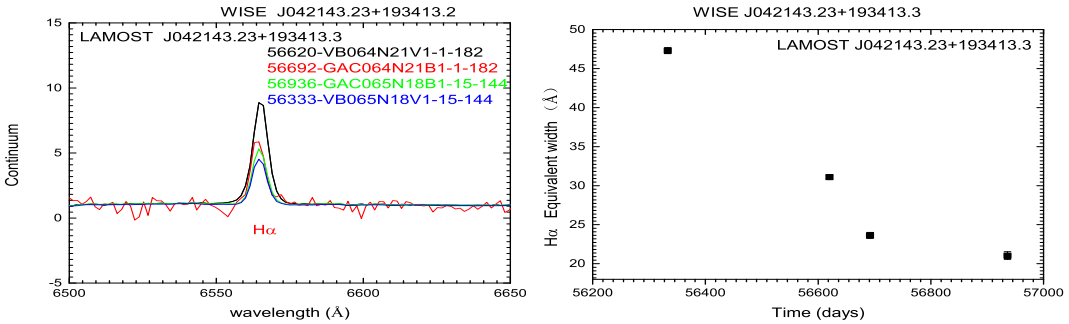

(a) LAMOST J042143.23+193413.3

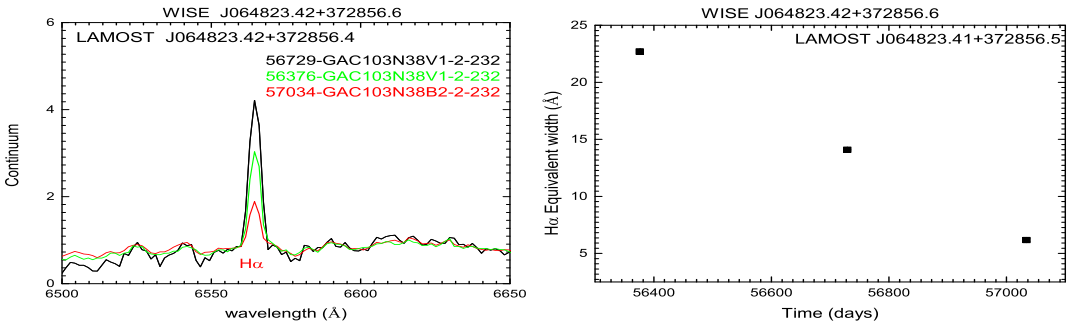

(b) LAMOST J064823.42+372856.6

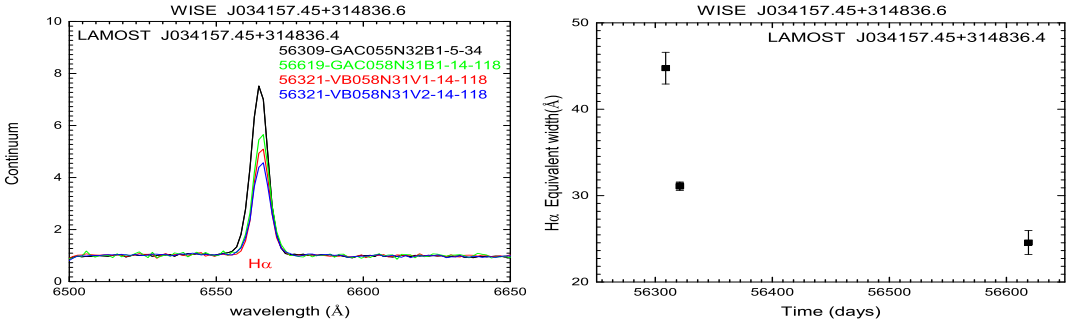

(c) LAMOST J034157.45+314836.4

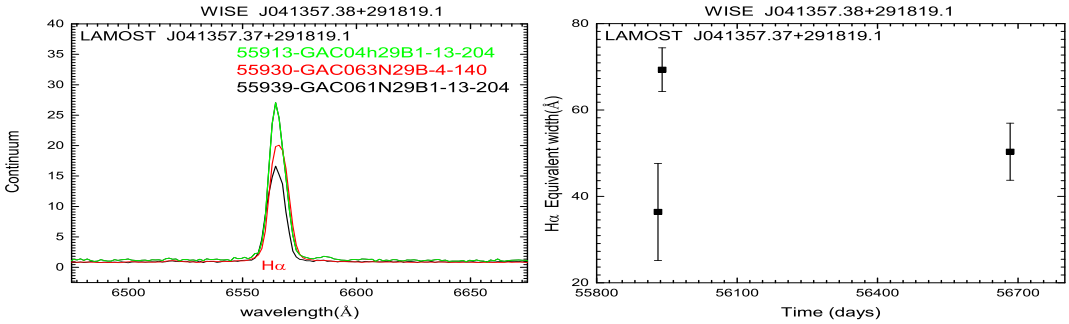

(d) LAMOST J0413573.37+291819.1

Figure 5. Samples of H alpha The equivalent width is variable.

Table 2. Infrared sources observed with LAMOST.

LAMOST Name (1)	Date (2)	S/N(u) (3)	S/N(g) (4)	S/N(r) (5)	S/N(i) (6)	S/N(z) (7)	W1(mag) (8)	W2(mag) (9)	W3(mag) (10)	W4(mag) (11)	Sp (12)	Survey (13)	Reference (14)
J093223.53+114603.1	2013-4-11	1.72	22.56	50.33	63.56	44.35	07.822	06.538	03.322	01.228	K4	konwn	Shin 2012
J093223.53+114603.1	2013-4-11	3.17	40.68	77.43	101.13	69.99	07.822	06.538	03.322	01.228	K5	konwn	Shin 2012
J094325.65+195139.8	2013-10-17	2.19	4.25	45.13	281.32	476.96	04.551	03.979	03.468	02.472	M8	konwn	Templeton 2005
J200748.93+460124.0	2012-10-2	7.17	60.67	126.91	190.61	160.96	07.799	07.408	04.113	02.127	K5	unkonwn	—-
J214144.88+024354.4	2014-11-19	2.56	6.41	10.9	15.36	10.95	05.571	05.634	05.619	05.536	A5	known	Li 2015
J231733.79+360020.0	2013-11-30	1.19	5.23	6.55	8.09	5.17	11.066	09.566	06.034	03.610		unkonwn	—-
J100149.52+284708.9	2014-1-29	1.41	2.96	8.59	12.33	7.13	11.066	09.566	06.034	03.610		konwn	Ichikawa 2017
J100149.52+284708.9	2012-11-23	2.39	28.5	80.83	231.66	253.19	06.600	06.354	04.883	04.003	M5	konwn	Ichikawa 2017
J101001.55-023743.2	2014-4-12	2.49	13.88	126.8	489.02	726.31	02.994	01.723	01.271	00.829	M8	konwn	Drake 2014
J201132.63+452203.5	2013-9-25	1.54	2.09	5.1	59.33	120.5	04.761	04.366	03.830	02.992	M8	unkonwn	—-
J202118.25+381243.9	2014-9-15	1.38	2.45	5.33	66.82	145.51	02.918	01.888	01.517	00.862	M8	konwn	Deguchi 2012
J234306.57+352845.3	2013-9-24	9.07	18.56	73.27	407.91	596.62	02.937	01.869	00.960	00.014	M7	konwn	Deguchi 2012
J134844.86+334334.3	2015-2-6	2.49	10.65	73.76	361.69	578.54	05.474	04.825	04.135	03.194	M7	konwn	Hübscher 2011
J140315.44+284139.0	2015-1-15	4.76	64.62	185.33	617.06	713.91	03.741	02.911	02.427	01.668	M5	konwn	Beers 1994
J143328.31+173646.9	2014-6-2	24.64	143.34	380.98	925	956.08	05.989	05.406	04.498	03.740	M4	konwn	Drake 2014
J225320.33+363028.5	2013-10-25	17.28	45.42	94.32	612.69	822.64	03.419	02.433	01.649	00.718	M7	konwn	Price 2010
J225632.27+363408.9	2013-10-14	8.07	52.31	173.12	520.14	679.46	04.785	04.390	04.001	03.301	M6	unkonwn	—-
J185758.05+430806.3	2013-10-4	2.28	10	68.48	377.62	547.37	04.661	03.776	03.251	02.627	M8	konwn	Coughlin 2014
J190026.57+382107.2	2014-6-2	1.83	5.53	4.04	3.26	2.92	10.265	09.258	04.119	02.487	A9	konwn	Richer 2017
J235954.26+565846.6	2014-11-20	0	30.43	243.59	375.45	404.98	05.434	04.599	04.227	03.991	M4	konwn	Alksnis 2001
J163348.93+295548.8	2014-3-12	2.55	28.94	67.38	97.11	74.65	06.088	06.238	06.140	06.032	K5	unkonwn	—-
J190419.10+501810.4	2015-5-30	1.8	49.29	148.52	323.9	308.95	06.748	06.992	06.776	06.660	M3	unkonwn	—-
J163511.86+372041.6	2012-4-25	5.3	21.21	105.11	438.01	610.96	03.109	02.189	01.479	01.188	M8	konwn	Weinberger 2015
J163511.86+372041.6	2012-3-31	2.07	7.62	15.56	82.65	113.78	03.109	02.189	01.479	01.188	M6	konwn	Weinberger 2015
J164018.21+384220.2	2012-3-31	1.71	2.8	4.21	4.33	2.08	13.180	12.359	07.762	03.590	A7	konwn	García-Hernández 2016
J190618.31+464458.9	2014-9-18	4.42	54.13	166.08	451.04	514.96	07.031	06.860	06.099	05.392	M6	konwn	Debosscher 2011
J164429.47+234801.9	2015-5-26	55.23	104.36	121.17	149.95	89	09.013	08.080	02.398		A1	konwn	Bear 2017
J230011.01-002251.6	2014-10-27	23.74	125.21	500.51	999	0	03.122	02.485	01.720	01.199		konwn	Price 2010
J190945.55+433653.2	2013-10-4	1.04	3.21	12.33	92.78	177.47	05.145	04.542	04.254	03.824	M8	konwn	Coughlin 2014
J190945.55+433653.2	2013-5-23	4.93	45.89	178.04	701.06	748.48	05.145	04.542	04.254	03.824	M4	konwn	Coughlin 2014
J191301.31+332448.6	2014-5-16	2.12	6.74	64.26	366.2	505.57	04.331	03.562	03.420	02.986	M8	konwn	Coughlin 2014
J191512.12+394250.5	2012-6-15	48.51	148.4	133.26	159.61	120.7	06.476	05.262	03.269	01.963	F7	konwn	Vega 2017
J170551.13+291321.9	2013-5-7	4.76	41.88	83.49	117.88	103.28	10.104	09.859	06.164	03.841	K4	konwn	Palla 1997

Note: Konwn said was also studied. Nnkonwn said was not also studied. We only show part of the infrared source observed with LAMOST of data in Table 1.

Through hammer program, we found 213 spectrums active stars with the Hα line, in which 116 spectrum have been observed multiple times. To distinction if the changed of multiple observation that chromospheric activity emitted the Hα lines. Our standards are the same as that of West (2011) and Zhang et al. (2016). Firstly the EWs of the Hα lines are no less than 1Å. Secondly the EW of the Hα line should be greater than the value of error. Thirdly the difference of the EW of the Hα line must be three times greater than the error. We found that 102 of them were variable. In Table 3, we shows part of the EW of the Hα lines.

Table 3. The equivalent width of the Hα line of star with multiple observation.

Same source	LAMOST name	WISE name	Spectral type	$H\alpha_{ew}$	$H\alpha_{error}$	Diff	S/N	Variable
12	J041749.65+282935.9	J041749.66+282936.1	M2	9.8925695	0.5173251	18.1496849	5.2774	Y
12	J041749.65+282936.2	J041749.66+282936.1	M5	7.1082635	0.0690321	17.3033504	32.9487	Y
12	J041749.65+282936.2	J041749.66+282936.1	M5	7.1082635	0.0690321	17.3033504	32.7982	Y
13	J041831.12+281628.4	J041831.13+281628.8	M0	81.6057892	1.0935481	162.5182953	22.1401	Y
13	J041831.12+281628.4	J041831.13+281628.8	M2	31.5187836	5.0577779	180.0876770	22.0534	Y
14	J041915.83+290626.9	J041915.83+290626.7	K4	27.0351562	2.3639345	151.5570831	21.5454	Y
14	J041915.83+290626.9	J041915.83+290626.7	M1	16.6940002	0.7525512	151.5680237	27.3470	Y
15	J042143.23+193413.3	J042143.23+193413.2	M5	31.0973053	0.2316574	11.7186966	9.1767	Y
15	J042143.24+193413.1	J042143.23+193413.2	M4	23.6203022	0.3863280	102.6457443	53.0280	Y
15	J042143.24+193413.1	J042143.23+193413.2	M3	21.0372410	0.5113782	88.4025040	46.2609	Y
15	J042143.23+193413.3	J042143.23+193413.2	M5	47.2996941	0.3964970	152.2059021	60.3708	Y
16	J042921.64+270125.7	J042921.65+270125.7	M2	5.5130100	0.1473798	9.3334055	22.3557	N
16	J042921.65+270125.6	J042921.65+270125.7	L1	45.0672035	14.0986404	61.1171722	15.6807	N
16	J042921.64+270125.7	J042921.65+270125.7	M8	53.1636848	14.3353949	41.7393112	13.0922	N
17	J042923.73+243300.2	J042923.73+243300.9	F4	52.8479309	2.1284502	21.2071342	4.2842	Y
17	J042923.73+243300.2	J042923.73+243300.9	K2	75.8311081	1.7166258	20.9036102	7.9231	Y
18	J043029.61+242644.9	J043029.62+242644.9	F4	52.8479309	2.1284502	21.2071342	47.1404	Y
18	J043029.61+242644.9	J043029.62+242644.9	M3	9.2656679	0.0069753	34.4671021	46.1454	Y
19	J043250.29+294239.5	J043250.30+294239.7	M5	3.9079747	0.0639671	7.0587926	11.4431	Y
19	J043250.29+294239.5	J043250.30+294239.7	L1	1.9316559	0.0164280	3.5155766	15.7561	Y
20	J043920.90+254502.1	J043920.92+254501.9	M2	72.6770935	0.4228196	85.8005447	13.3346	Y
20	J043920.92+254501.8	J043920.92+254501.9	M1	66.7842712	1.5345556	112.3731613	16.8842	Y
21	J044621.78+172303.1	J044621.81+172303.5	M6	13.9664001	0.0786490	15.5491953	8.2714	Y
21	J044621.78+172303.1	J044621.81+172303.5	M5	12.4391394	0.0541400	13.8067837	8.3747	Y
22	J044813.48+292453.5	J044813.48+292453.5	M2	20.6756344	0.6101283	82.8008499	54.1792	Y
22	J044813.48+292453.4	J044813.48+292453.5	M3	24.5430584	0.8001958	85.0495377	32.9934	Y
23	J053002.04+121335.8	J053002.01+121335.7	G8	20.8385754	0.1733870	42.1097870	12.6016	Y
23	J053002.02+121335.6	J053002.01+121335.7	K5	35.2215080	0.0241762	126.6769943	23.2903	Y
24	J053128.05+120910.2	J053128.05+120910.2	G3	86.7132111	1.5561818	63.1558456	10.5369	Y
24	J053128.04+120910.3	J053128.05+120910.2	F7	59.1888199	0.0341495	338.5122681	41.1235	Y
25	J053200.30-045553.8	J053200.30-045553.8	B0	12.6712179	0.0950776	13.6715822	25.7179	Y
25	J053200.30-045553.8	J053200.30-045553.8	B0	10.2123613	0.1399300	11.9934368	24.0989	Y
26	J053209.94-024946.7	J053209.94-024946.7	K4	4.1657314	0.0019114	62.8156776	53.8309	Y
26	J053209.94-024946.7	J053209.94-024946.7	K4	7.3370047	0.0029331	52.7106781	54.0553	Y
27	J053415.74-063604.6	J053415.74-063604.5	K3	2.4419281	0.0243778	12.2068777	62.9769	Y
27	J053415.74-063604.6	J053415.74-063604.5	K3	2.5272474	0.0149375	12.7578421	33.6247	Y
28	J060205.78-011428.3	J060205.78-011428.2	G9	21.6452446	0.0564436	71.3180771	10.0462	Y
28	J060205.78-011428.3	J060205.78-011428.2	G9	15.6448870	0.0380235	46.7075233	14.9352	Y

Note:Y means that the activity of the star is variable,N means that the activity of the star is not variable

3.4 Chromospheric Activity

The physical mechanism of spectral emission from early and late stars are different. The early-type stars (Oe, Ae and Be), which evolve from dense molecular clouds, has its accretion of dust disks, stellar winds and rapid rotation, leading its Hα emission line originating from the outer atmosphere of the star or stellar envelopes (Golden-Marx et al., 2016; Hou et al., 2016; Ahmed & Sigut, 2017). The early-type stars with the Hα emission line have 25 infrared source in our sample. The late-type stars produces a spectrum of a series of emission lines (Balmer lines, Ca II H&K and Ca II IRT). These activity magbe

due to the stellar chromospheric activity and magnetic activity caused by plage and flare (Zhang et al., 2015; Zhang et al., 2016; Vida et al., 2015; Montes & Crespo-chacón, 2004).

4 Summary

(1) LMAOST and WISE cross-certification have obtained 3762 stars from 158114 infrared stars and 2184 stars from 145905 infrared galaxies.
(2) According to the spectra of active stars emits in the Hα, Hβ, Hδ, Hγ, Ca II H&K, and Ca II IRT band. We have obtained 390 active stars.
(3) We studied the 390 spectrum of stars and found 77 of them are first observed by LAMOST.
(4) With the help of the equivalent width of the Hα line obtained by the hammer program, We verified that 102 spectra of active stars are variable.

Acknowledgments. This research is supported by the Joint Fund of Astronomy of the NSFC and CAS Grant Nos. 11963002 and U1931132. Guoshoujing Telescope (the Large Sky Area Multi-Object Fiber Spectroscopic Telescope LAMOST) is a National Major Scientific Project built by the Chinese Academy of Sciences.

References

1. Ahmed, A., Sigut, T. A. A., 2017. MNRAS 471, 3398A.
2. Aumann H. H., et al., 1984. ApJ 278, L23.
3. Covey, K. R., Ivezié,Ż., et al., 2007. AJ 134, 2398.
4. Catalano, S., Lanza, A. F., et al., 1998. ASPC 154,584.
5. Cui, X. Q., Zhao, Z. H., et al.,2012. RAA 12, 9, 1197.
6. Dhital, S., West, A. A., et al., 2012. AJ 143,67.
7. Egan M. P., Shipman R. F., Price S. D., Carey S. J., Clark F. O., Cohen M., 1998, ApJ 494, L199
8. Frasca, A., Molenda-Żakowicz, J., et al., 2016. A&A 594, 39.
9. Golden-Marx, Jesse B., Oey, M. S and Lamb, J. B., et al., 2016. APJ 819, 55G.
10. Hou, Wen., Luo, A. Li and Hu, Jing-Yao., 2016. RAA 16,138H.
11. Hawley, S. L., Covey, K. R., Knapp, G. R., et al., 2002. AJ 123,3409.
12. Koenig, X., Hillenbrand, L. A.,et al.,2015,AJ,150,100K
13. Koenig, X. P., Leisawitz, D. T., Benford, D. J., et al., 2012. ApJ 744, 130K
14. Lee, Y. S., Beers, T. C., et al., 2008. AJ 136, 2022.
15. Luo, A. L., Zhang, H. T., et al., 2012. RAA, 12, 9, 1243.
16. Montes,D., Crespo-chacón., et al., 2004. LNEA 1, 119.
17. Oudmaijer, R. D., van der Veen, W. E. C. J., Waters, L. B. F. M., et al. 1992, A&A, 96, 625
18. Perault, M., et al., 1996. A&A 315, L165
19. Peretto, N., Fuller G. A., 2010. ApJ 723, 555
20. Rhee, J. H., song I R. zuckerman, B, et al. 2007, ApJ 660, 1556
21. Rathborne J. M., Jackson J. M., Simon R., 2006, ApJ 641, 389
22. Vida, K., Korhonen, H., et al., 2015, A&A, 580, 64.
23. West, A. A., Morgan, D. P., et al., 2011. AJ 141, 97.
24. Wright, Edward, L., Eisenhardt, Peter, R. M., et al., 2010. AJ 140, 1868.
25. Woolf, V. M., West, A. A., 2012, MNRAS, 422, 1489.
26. Yi, Z. P., Luo, A. L., et al., 2014. AJ 147, 32.
27. Zhang, L. Y., Pi, Q. F., et al., 2015. RAA 15, 252.
28. Zhao, G., Zhao, Z. H., et al., 2012. RAA 12, 7, 723.
29. Zhang, L. Y., Pi, Q. F., et al., 2016. NewA 44, 66.

